buildings

Article

Yielding and Ultimate Deformations of Wide and Deep Reinforced Concrete Beams

Fernando Gómez-Martínez and Agustín Pérez-García

Special Issue

Advanced Research and Prospect of Buildings Seismic Performance

Edited by
Dr. Rafael Shehu , Dr. Nicola Tarque and Dr. Manuel Buitrago

Article

Yielding and Ultimate Deformations of Wide and Deep Reinforced Concrete Beams

Fernando Gómez-Martínez [1,*] and Agustín Pérez-García [2]

1   Department of Structural Mechanics and Hydraulic Engineering, Universidad de Granada, Campus Fuentenueva S/N, 18071 Granada, Spain
2   Department of Mechanics of the Continuum Media and Theory of Structures, Universitat Politècnica de València, Camí de Vera, S/N, 46022 Valencia, Spain
*   Correspondence: fergomar@ugr.es

Abstract: Current formulations proposed by Eurocode 8 part 3 for the inelastic deformations of existing reinforced concrete members are assessed separately for wide beams (WB) and conventional deep beams (DB). The current approach, based on a large experimental database of members, predicts larger ultimate chord rotation but lower chord rotation ductility for WB rather than for DB despite the similar curvature ductility, due to lower plastic hinge lengths in WB. However, if the data are disaggregated into DB and WB, predicted chord rotations are consistently conservative for DB and not conservative for WB if compared with experimental values, especially at ultimate deformation. Thus, plastic hinge length may be even greater for DB in comparison to WB. Therefore, some feasible corrections of the formulations for chord rotations are proposed, in order to reduce the bias and thus increase the robustness of the model for cross-section shape variability.

Keywords: wide beams; deep beams; chord rotation; ductility; plastic hinge length; Eurocode 8

1. Introduction

Wide beams are defined by their cross-section aspect ratio in which the width is larger than the depth, and typically also larger than the column dimensions. Their use as an alternative to conventional deep beams in reinforced concrete (RC) frames is quite widespread in seismic regions of the Mediterranean area [1–5]. Traditionally, seismic codes have imposed severe restrictions on the use of wide-beam frames (WBF), such as limitations to their use in high seismicity areas or reduction in behaviour factor (*q*) [6–8]. However, most of current codes dispense similar treatment to WBF as to deep-beam frames (DBF), except for some geometric and mechanical limitations regarding beam–column connections, mainly the ratio between the beam width and the column dimensions. These restrictions have been demonstrated to guarantee proper local performance, as observed in several experimental and analytical tests of wide beam–column sub-assemblages [9–19].

In [7,8], it is shown that WBF may provide similar seismic global performances to DBF when both are designed according to modern performance-based seismic codes such as Eurocode 8 part 1 (EC8-1) [20]. Despite lower local ductility of WB with respect to DB, WBFs show higher effective stiffness and deformation capacity, thanks especially to code provisions regarding the damage limitation limit state. There are some other mechanical benefits of WBF with respect to DBF: higher shear span in first-storey columns, higher ultimate chord rotation of beams, and lower deformability of joints.

Nevertheless, the similar treatment of WBF and DBF in current codes requires an accurate estimation of inelastic deformations of WB under cyclic loads, because the overall performance of the whole structure relies on their member ductility, among other characteristics concerning capacity design. For this aim, some performance-based seismic codes such as the American ASCE-SEI/41-06 (ASCE in the following) [21] or the European Eurocode 8

part 3 (EC8-3) [22] provide different expressions for yielding and ultimate chord rotation capacity of members. The model of EC8-3 is based on a continuous work developed in [23–26]. These formulations are obtained as a regression of experimental results contained in an increasing database up to 1540 tests. However, only 37 of those elements are WB, so it is not clear whether those formulations can appropriately fit those elements.

The scope of this paper is to evaluate the reliability of the current deformation model adopted by EC8-3 regarding wide beams. Firstly, a comparative numerical analysis of curvatures and chord rotations of a parametric set of eight couples of WB and DB was carried out, in which both current European and American approaches were used in order to understand the different cross-sectional behaviours and the corresponding inelastic member performances. Then, the experimental results of the database on the basis of the EC8-3 approach were disaggregated into DB and WB, and current formulations were applied separately in order to find whether experimental-to-predicted ratios are biased or not for both groups. Finally, some corrections for the current formulations are proposed in order to reduce the bias and thus increase the robustness of the model against cross-sectional shape variations.

2. Numerical Comparison of Deformations of Wide and Deep Beams

Inelastic flexural deformation of members is typically characterised by chord rotation θ at yielding and ultimate deformation (θ_y and θ_u, respectively). Macroscopic value θ is related to local variables, i.e., cross-section curvatures at yielding and ultimate deformation (ϕ_y and ϕ_u, respectively), through shear span (L_V) and plastic hinge length (L_{pl}). In all the following, b_w and h_b are cross-section width and height, respectively; c_n, concrete cover; d, effective depth; d', distance from extreme fibres to the axe of reinforcement; z, internal lever arm; x, neutral axis depth; d_{bL} and d_{bt}, mean diameter of longitudinal and transverse reinforcement, respectively; A_{s1} and A_{s2}, tensioned and compressed reinforcement areas, respectively; ω, ω', and ω_{tot}, bottom, top, and total mechanical reinforcement ratio, respectively; ρ_w, transverse reinforcement ratio; f_c, resistance of concrete; f_y and f_u, yielding and ultimate steel strength, respectively; and M_y and M_u, yielding and ultimate bending moment, respectively. For any parameter A, ratios between values corresponding to WB and DB are indicated as $A_{W/D}$ (rather than using the heavier notation A_{WB}/A_{DB}).

In general, the elastic stiffness of WB is lower than for DB due to $h_{b,W/D} \leq 1$, although $b_{w,W/D} \geq 1$; thus, post-cracked deformability may also be expected to be higher for WB than for DB. In terms of curvature ductility μ_ϕ, traditionally WBs are considered to provide lower values than DBs [4,27], i.e., $\phi_{u,W/B} \leq \phi_{y,WB}$. This statement is based on generic considerations: when h_b is reduced, higher A_{s1} is required; thus, a large, compressed concrete area is needed in order to satisfy equilibrium, which sometimes can be only attained by means of higher x, likely causing higher ϕ_y and lower ϕ_u, and thus lower μ_ϕ. However, such an argument does not take into account that $b_{w,W/D}$ can be quite large, nor that sections designed as high ductility class (DCH) perform as confined ones. On the other hand, it is difficult to find explicit and systematic comparative analyses in the literature for WB and DB regarding θ instead of ϕ. In fact, code provisions guarantee enough member (chord rotation) ductility μ_θ by implicitly regulating μ_ϕ, without any consideration regarding L_{pl} depending on the cross-sectional aspect ratio.

In Appendix A, preliminary generic considerations aimed at estimating cross-sectional and member ductilities for DB and WB designed in DCH are carried out, taking into account the previous conditions. In that scenario, cross-sectional behaviour can be interpreted as shown in Figure 1: thanks to the confinement, similar ductilities are expected for both types, which is a different conclusion than what is found in the literature. The main reason is that ultimate deformation is ruled by the tensioned steel rather than the failure of compressed concrete; thus, both yielding and ultimate curvature ratios are rather inversely proportional to the depth ratios of the beams.
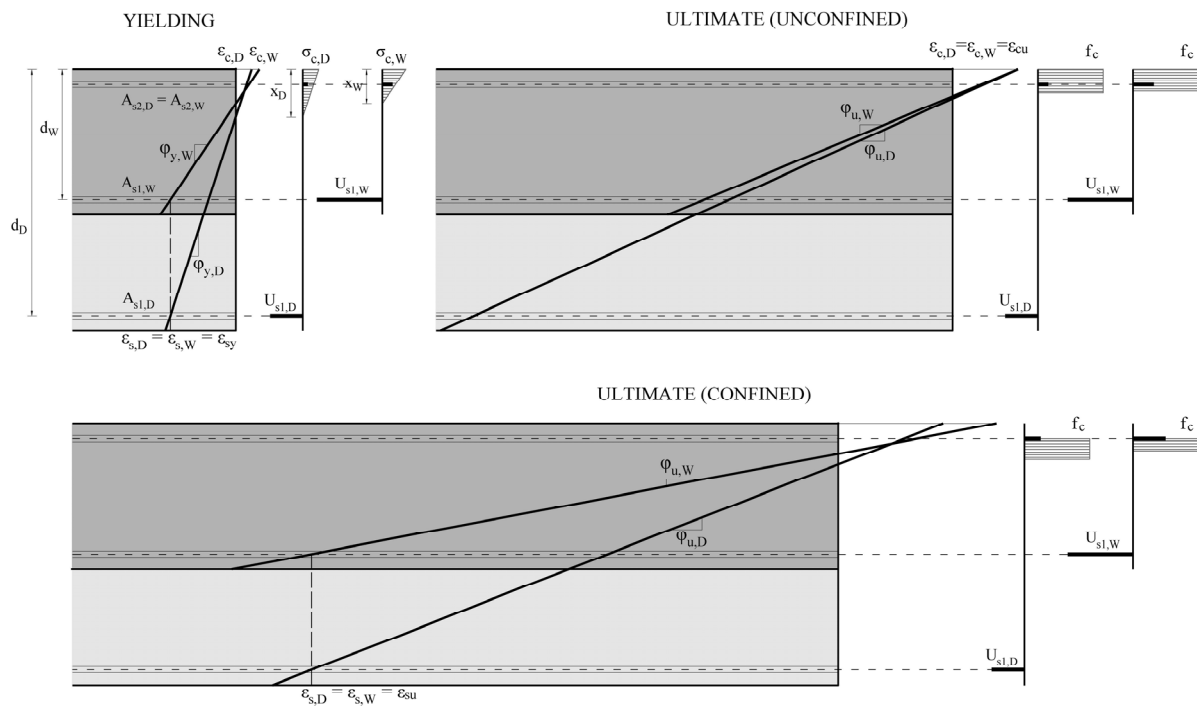
Figure 1. Simplified comparison between curvatures of generic WB (dark grey) and DB (depth increment in light grey) for yielding and ultimate deformations for confined and unconfined cases.

On the other hand, aimed at an estimation of $\mu_{\theta,W/D}$, two main code-based procedures for obtaining θ can be considered: EC8-3 and ASCE. EC8-3 proposes explicit formulations for θ_y and θ_u. θ_y expression (Equation (1)) depends mainly on ϕ_y, being a_v a zero-one parameter for pre-yielding shear concrete cracking. For θ_u, two approaches are proposed: one with a more fundamental basis (Equation (2)), depending on constant $\phi_{pl} = \phi_u - \phi_y$ alongside L_{pl} (calculated as in Equation (3)), and two pure empirical expressions, the first one explicitly for θ_u (Equation (4)) and a second one furnishing values of θ_{pl}, which is not considered in this work. α is the confinement effectiveness factor, ω_w the transverse mechanical reinforcement ratio, and ρ_d the diagonal reinforcement ratio. Only formulations for members without lap-splices in reinforcement are considered, as lap-splices are recommended to be placed outside critical regions for beams designed for high ductility [28].

$$\theta_{y,EC8} = \phi_y \left(\frac{L_V + a_v z}{3} + 0.13 d_{bL} \frac{f_y}{\sqrt{f_c}} \right) + 0.0013 \left(1 + 1.5 \frac{h_b}{L_V} \right) \tag{1}$$

$$\theta_{u,EC8,fun} = \theta_{y,EC8} + \left(\phi_u - \phi_y \right) L_{pl,EC8} \left(1 - \frac{L_{pl,EC8}}{2L_V} \right) \tag{2}$$

$$L_{pl,EC8} = 0.03 L_V + 0.2h + 0.11 d_{bL} \frac{f_y}{\sqrt{f_c}} \tag{3}$$

$$\theta_{u,EC8,emp} = 0.016 \left(\frac{\max\{0.01; \omega'\}}{\max\{0.01; \omega\}} f_c \right)^{0.225} \left(\frac{L_V}{h_b} \right)^{0.35} \cdot 25^{\alpha \omega_w} \cdot 1.25^{100\rho_d} \tag{4}$$

Concerning the argument of which type of approach is more suitable, pure empirical or more fundamental, two considerations must be made. Firstly, inelastic behaviour of RC members is a complex phenomenon which is difficult to model satisfactorily from a pure theoretical point of view [27]; in fact, in this specific case empirical model is intended to provide more reliable predictions, showing higher robustness to the variability of single parameters [26,29]. Secondly, and more importantly, is it worth noting that the more fundamental approach is not a pure fundamental one. It adopts an apparent the-

oretical framework (Equation (2)) but then adds a yielding contribution which contains pure empirical factors to a plastic contribution which depends on a plastic hinge length whose calculation is also purely empirical (Equation (3)). Hence, it is actually another empirical expression.

Conversely, in the ASCE procedure, θ_y (shown in Equation (5) only for flexural deformation) is obtained indirectly as M_y/K_{sec} (K_{sec} being the secant-to-yielding member stiffness, obtained as a constant fraction of gross uncracked one taking into account also shear contribution). θ_u is obtained as $\theta_y + \theta_{pl}$, where the plastic contribution $\theta_{pl} = \theta_u - \theta_y$ is picked from Table 1, being s_t the stirrup spacing, V_s the stirrup shear strength contribution, V_{pl} the maximum shear corresponding to the attainment of moment resistances, and ρ_{bal} the reinforcement ratio for balanced strain conditions.

$$\theta_{y,ASCE} = \frac{M_y L_V}{3(0.3 E_c I)} \tag{5}$$

Table 1. Values of $\theta_{pl,ASCE}$.

$s_t < d/3$ and $V_s > 0.75V_{pl}$	$\frac{\rho - \rho'}{\rho_{bal}}$	$\frac{V_{pl}}{b_w d \sqrt{f_c}}$	$\theta_{pl,ASCE}$
(Y/N)	-	-	(rad)
Y	≤ 0.0	≤ 3	0.025
		≥ 6	0.020
	≥ 0.5	≤ 3	0.020
		≥ 6	0.015
N	≤ 0.0	≤ 3	0.020
		≥ 6	0.010
	≥ 0.5	≤ 3	0.010
		≥ 6	0.005

As shown in Appendix A, fundamental and experimental approaches return different member ductilities for WB and DB. According to the fundamental one, rather similar ductilities to those corresponding to curvatures are expected, while the experimental method furnishes lower ductilities for WB.

If results of the empirical approach are interpreted similarly to the fundamental approach, i.e., as the consequence of plastic curvatures alongside plastic hinge length, it is possible to obtain equivalent implicit values of $L_{pl,eq,W/D} \approx \theta_{u,W/D}/\phi_{u,W/D}$, again neglecting yielding deformations with respect to ultimate ones. It results in values of $1/(b_{w,W/D} \cdot d_{W/D}^{1.35})$ for unconfined beams and $d_{W/D}^{0.65}$ for confined ones, which means that WB may show shorter $L_{pl,eq}$ than DB for confined sections but higher values in the unconfined case, which is contrary to the trend observed in most of the expressions proposed for plastic hinge length [23,26,27].

The ASCE method may provide different values than EC8-3, as it is not based on curvatures. $\theta_{y,W/D}$ only depends on gross stiffness, which may return large differences between WB and DB. On the other hand, θ_{pl} for design in DCH may be rather similar in all the cases, as it depends mainly on the stirrup arrangements; however, provided values are independent of geometry, so it may not be possible to predict corresponding ratios for θ_u and μ_θ.

Hence, within the limitations of these preliminary simplified considerations, in general, WBs designed in DCH are expected to provide similar curvature ductilities but chord rotation ductilities lower than or similar to DBs. It is worth noting that such relationships seem to depend mainly on cross-section dimensions.

Aimed at a proper assessment of those preliminary conclusions, a systematic analysis is required. In this section, the set of eight couples of WB and DB already used in [7] is adopted, aimed at a comparative numerical analysis of deformations, but in this case,

the contribution of confinement is considered alternatively as null and complete. The actual comparison between DB and WB is based on both magnitudes ϕ and θ, and the corresponding ductilities (μ_ϕ and μ_θ) are also obtained. The characteristics of the set of beams are presented in Table 2, assuming $L_V = 2.5$ m, $c_n = 20$ mm, $d_{bL} = 14$ mm, $d_{bt} = 8$ mm, $f_c = 33$ MPa, and $f_y = 630$ MPa.

Table 2. Characteristics of the analysed set of beams.

Class of Beam	Section Type	Geometry		Transverse Reinforcement		Longitudinal Reinforcement									
							Low				High			
							$\omega'/\omega = 1.5$		$\omega'/\omega = 1$			$\omega'/\omega = 1.5$		$\omega'/\omega = 1$	
		b_w	h_b	Hoops	ρ_w	ω_{tot}	Reinf. Ratio	M_y	Reinf. Ratio	M_y	ω_{tot}	Reinf. Ratio	M_y	Reinf. Ratio	M_y
		(mm)	(mm)	(mm)	(%)	(-)	(%)	(kNm)	(%)	(kNm)	(-)	(%)	(kNm)	(%)	(kNm)
DB	A	300	600	2φ8/70	0.48	0.10	$\rho' = 0.30$ $\rho = 0.20$	−181 +122	0.25	±152	0.29	$\rho' = 0.90$ $\rho = 0.60$	−524 +357	0.75	±442
	B	300	500				$\rho' = 0.30$ $\rho = 0.20$	−124 +84	0.25	±104		$\rho' = 0.90$ $\rho = 0.60$	−357 +244	0.75	±301
WB	A	650	300	4φ8/70	0.44	0.19	$\rho' = 0.60$ $\rho = 0.40$	−177 +120	0.50	±149	0.60	$\rho' = 1.89$ $\rho = 1.26$	−513 +362	1.50	±446
	B	500	300		0.57	0.17	$\rho' = 0.54$ $\rho = 0.36$	−123 +83	0.45	±103	0.53	$\rho' = 1.65$ $\rho = 1.10$	−355 +244	1.38	±301

Five parameters are assumed: (i) class (DB or WB); (ii) cross-sectional aspect ratio (h_b/b_w) for each class (types A and B, providing higher or lower M_y, respectively); (iii) $\omega'/\omega = 1$ or 1.5, which in most cases satisfy the requirements of EC8 for DCH; (iv) ω_{tot} (high and low, which makes top and bottom reinforcement, respectively, correspond to code's upper and lower limit when $\omega'/\omega = 1.5$); and (v) effectiveness of transverse reinforcement on confinement (yes or no). DB and WB show similar M_y for each case, and the high reinforcement case provides approximately three times the flexural strength provided by low reinforcement. Stirrup arrangements satisfy the requirements for DCH of EC8 and also the limitations provided by Eurocode 2 (EC2) [30] regarding the number of transverse legs.

2.1. Curvatures

Full moment–curvature (M-ϕ) relations are obtained through a fibre model for all the cases. Eurocode-based strain–stress models are assumed. For concrete, an EC2 parabolic envelope and confinement model proposed in EC8 are adopted. For steel, a bilinear envelope with hardening is considered, with values of f_u/f_y and ultimate strain ε_{su} according to those suggested in EC2 for steel type B.

Results for confined cases with asymmetric longitudinal reinforcement are shown in Figure 2. Post-elastic hardening of reinforcement causes that in most cases, $M_u > M_y$. In almost all the cases, there is spalling of concrete cover before the attainment of ε_{su} in the tension reinforcement, causing an instantaneous slight drop of M. Hence, $\phi_u$of WB reaches larger values than DB, as predicted. It is worth noting that the increment in secant-to-yielding stiffness for high-reinforced sections with respect to low-reinforced ones is rather similar to such an increment in total reinforcement.

In most cases, simplified assumptions made in the preliminary considerations (pre-emptive yielding of steel, concrete and steel failure in unconfined and confined sections, respectively, quasi-linear behaviour of concrete until ϕ_y, negligible values of x with respect to d, similar top reinforcement stresses at ϕ_y, etc.) are confirmed, and estimated values of ϕ and μ_ϕ are predicted with error lower than 10%. In Figure 3, one of the couple DB-WB is studied in detail. It corresponds to a case in which WB presents approximately half the depth and double the width of DB; thus, the cross-sectional area is rather similar. The

results confirm the predictions: WB shows double ϕ_y, similar $\phi_{u,unconf}$, and more than double $\phi_{u,unconf}$ compared to DB.
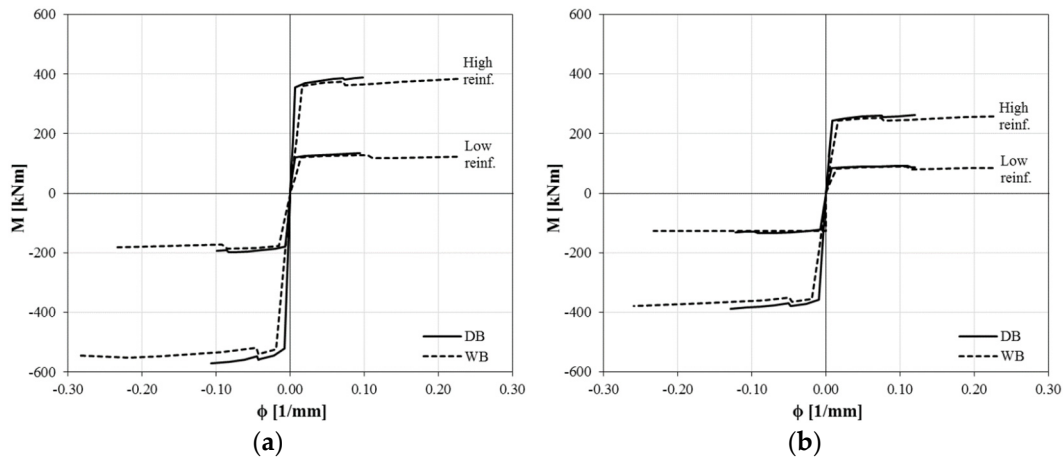

Figure 2. M−φ relations for the confined cases of the parametric set of beams corresponding to $\omega'/\omega = 1.5$, for (**a**) section types A and (**b**) section types B.
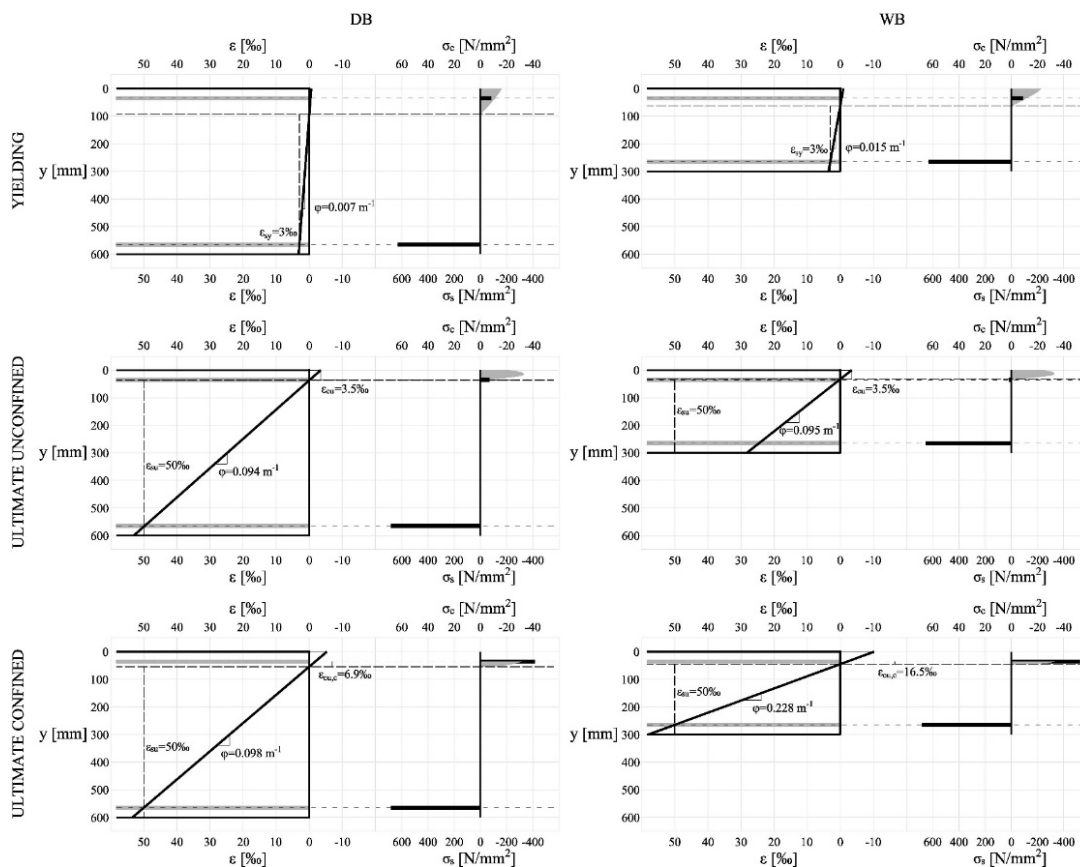

Figure 3. Cross-sectional strain and stress distribution for positive flexure of DB and WB type A, high reinforcement, and $\omega'/\omega = 1$ of the parametric set of beams.

Results for all the cases are shown in Figure 4, in which mean ratios between WB and DB are indicated as W/B in the bottom of the graphics. In general, more satisfactory values are obtained for asymmetric reinforced sections in positive bending than in the rest. For unconfined cases, high-reinforced sections show much poorer performances in terms of μ_ϕ

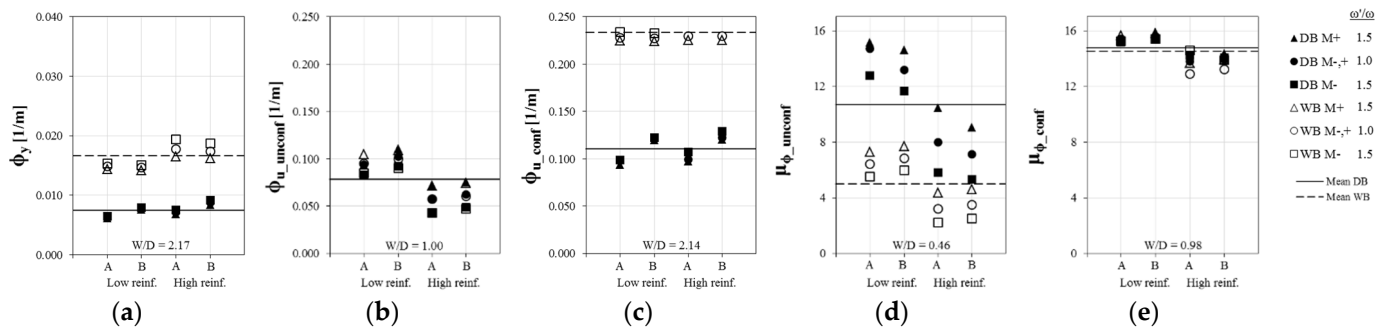than low-reinforced sections (almost half values), while for confined sections, the bias is much lower.

Figure 4. (**a**) ϕ_y; (**b**) ϕ_u for unconfined case; (**c**) ϕ_u for confined case; (**d**) μ_ϕ for unconfined case; and (**e**) μ_ϕ for confined case in all the beams of the parametric set.

It is worth noting that provisions of EC2 regarding the distribution of stirrup legs within the width of the section causes quite a higher contribution of confinement in WB rather than in DB: in terms of $\mu\phi$, DB is multiplied by 1.5 on average, while for WB, the factor is almost 3.0. Even in the cases of asymmetric high-reinforced WB to negative bending, which does not satisfy DCH provisions on longitudinal reinforcement, high confinement causes similar values of $\mu\phi$ than in the rest of the cases.

2.2. Chord Rotations

EC8-3 and ASCE procedures are carried out for all the cases. Regarding the first approach, θ_y(Figure 5a) shows a similar relative distribution of values to ϕ_y, although $\theta_{y,W/D}$ is 15% lower than $\phi_{y,W/D}$ on average due to the different shear contribution at yielding, independent of curvature. Mean secant-to-yielding stiffness values are on average 9% and 23% of the uncracked gross stiffness for low- and high-reinforced DB, respectively, and 15% and 38% for WB, respectively, due to the higher reinforcement ratios in WB than in DB. The mean global value is 21%, consistently with [23].
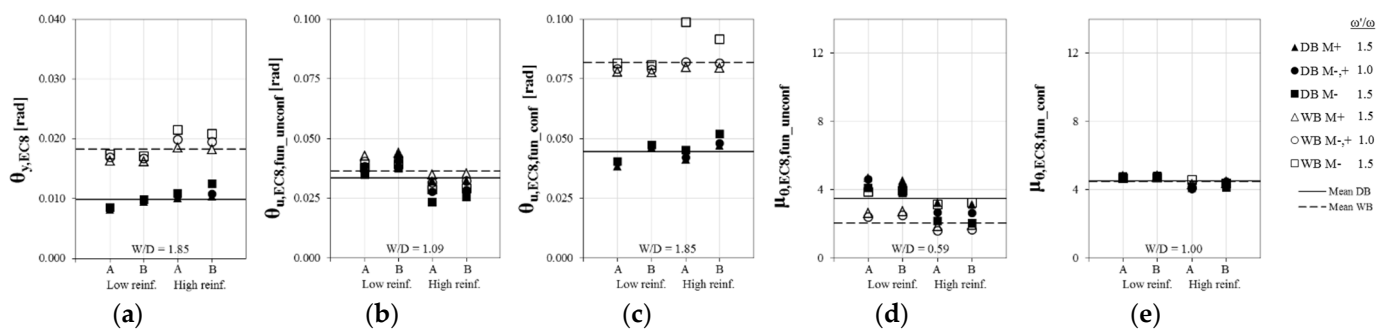

Figure 5. (**a**) θ_y; (**b**) θ_u for unconfined case; (**c**) θ_u for confined case; (**d**) μ_θ for unconfined case; and (**e**) μ_θ for confined case in all the beams of the parametric set according to EC8-3 fundamental approach.

In Figure 5b,c, θ_u values for unconfined and confined cases, respectively, obtained following the EC8-3 fundamental approach, are shown. L_{pl} of WB is 0.86 times that of DB, on average. This is exactly the ratio between mean values of $\theta_{u,W/D}/\phi_{u,W/D}$ for confined beams (see Figures 4c and 5c); however, for unconfined beams, still larger θ_u values for WB rather than for DB are shown, notwithstanding the lower L_{pl} for WB, because in this case, large yielding deformations are not negligible with respect to ultimate ones. Consequently, μ_θ is 40% lower for WB rather than for DB for the unconfined section, while similar ductilities are expected for confined beams (see Figures 5d and 5e, respectively).

Figure 6a,b corresponds to θ_u for unconfined and confined cases, respectively, obtained following the EC8-3 empirical approach. The relative positive influence of confinement on WB is quite lower than for the fundamental approach: the mean increment in θ_u is only 16% instead of 125%. For unconfined beams, notwithstanding the similar ϕ_u for WB and DB, higher values of θ_u are observed for WB rather than for DB; in fact, the implicit equivalent plastic hinge length is 32% higher for WB, on average. Instead, for confined cases, mean $L_{pl,eq,W/D} = 0.62$, which is more consistent with explicit values within the fundamental approach. The lower influence of confinement on WB causes that, even on confined beams, μ_θ is 25% lower for WB than for DB.
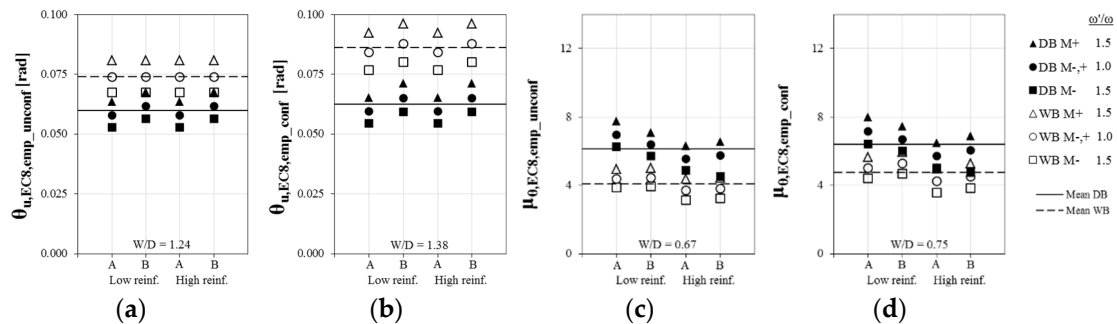

Figure 6. (**a**) θ_u for unconfined case; (**b**) θ_u for confined case; (**c**) μ_θ for unconfined case; and (**d**) μ_θ for confined case in all the beams of the parametric set according to EC8-3 empirical approach.

Finally, in Figure 7b,c, θ_u values for unconfined and confined beams, respectively, corresponding to the ASCE approach, are presented. Values of θ_y (Figure 7a) correspond by definition to a constant degradation of 30% from the uncracked gross stiffness; thus, much larger differences between high- and low-reinforced sections are observed. Values are much lower (about half times) than in both EC8-3 approaches for confined cases, because within this method, increment due to confinement is very low. The differences in θ_u between the different cases are only due to the contribution of θ_y, because values of θ_{pl} are rather constant for all the beams. It is worth noting that similar mean ratios between $\theta_{u,W/D}$ for confined sections are obtained with ASCE and EC8-3 empirical approaches: about 1.37. According to the ASCE approach, WB shows less than half the μ_θ of DB (see Figure 7d,e).
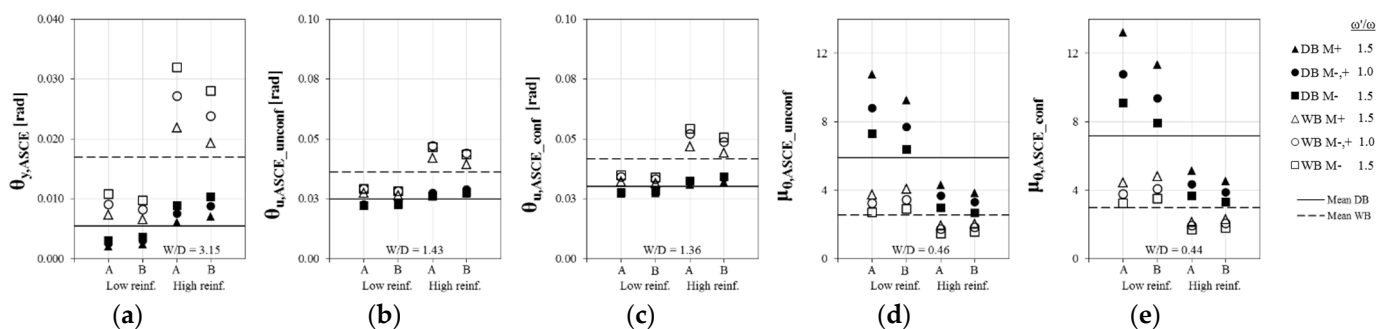

Figure 7. (**a**) θ_y; (**b**) θ_u for unconfined case; (**c**) θ_u for confined case; (**d**) μ_θ for unconfined case; and (**e**) μ_θ for confined case in all the beams of the parametric set according to ASCE.

3. Disaggregation of Experimental Database

Affirming the reliability of the results obtained in the previous section requires the EC8-3 method to be appropriate, aimed at predicting deformations of WB. In this section, those formulations are assessed at this scope.

The EC8-3 approach has almost fully adopted the formulations corresponding to members under cyclic loading, with proper seismic design and with potential slippage of longitudinal bars, proposed in [25,26] for deformations at yielding and ultimate, respectively. All those expressions are obtained as a regression of experimental results

contained in a large database of about 1540 tests [24]; for more detailed information on the composition of the database, see Appendix B.

The current paper only considers beams with a full rectangular cross-section and ribbed bars, with neither lap-splices nor precompression or retrofitting, whose failure is governed by uniaxial flexure. Hence, 277 DB and 37 WB are selected. Regarding wide cross-sections, only 5% of the total amount of specimens are tested in the parallel direction to the cross-section axe of minimum stiffness (members oriented as "wide" sections). Hence, the reliability of the models based on such databases for this minority might be under discussion.

For this aim, the model by Biskinis and Fardis [25,26]—B&F in the following—and also the preliminary one by Panagiotakos and Fardis [23]—P&F in the following—are applied separately to the sub-databases of DB and WB, in order to obtained disaggregated values of experimental-to-predicted ratios and thus assess the possible bias of results within the two groups. The ASCE model is also employed in order to compare the accuracy regarding WB and DB, although it is actually regressed from another database [31]. The results of the disaggregated application of deformation models should be carefully considered considering that the sub-database of WB is quite reduced and also unbalanced regarding the previous items.

All the graphics presented in the following show (i) the median value—which is intended to be more representative than the mean in the case of large dispersion [23]—of single experimental-to-predicted ratios, which is indicated as "Median exp/pred" and which corresponds to the slope of the plotted thick line; (ii) the 16th and 84th percentiles (associated with standard deviation in a normal distribution), corresponding to the slope of the dashed lines; and (iii) the coefficient of variation (CoV).. It is also indicated in each case which half of the graphic corresponds to conservative results (i.e., when formulations provide overestimation at yielding and underestimation at ultimate deformation).

3.1. Curvatures

Stress–strain models are similar to those adopted in the original approach (see Appendix B). Experimental and predicted ϕ_y (through the fibre model) are compared in Figure 8a,b for DB and WB, respectively. In both cases, adequate fitting is shown, although the fibre model slightly underestimates values. Rather similar trends are obtained if the simplified procedures in [23,25] are performed.
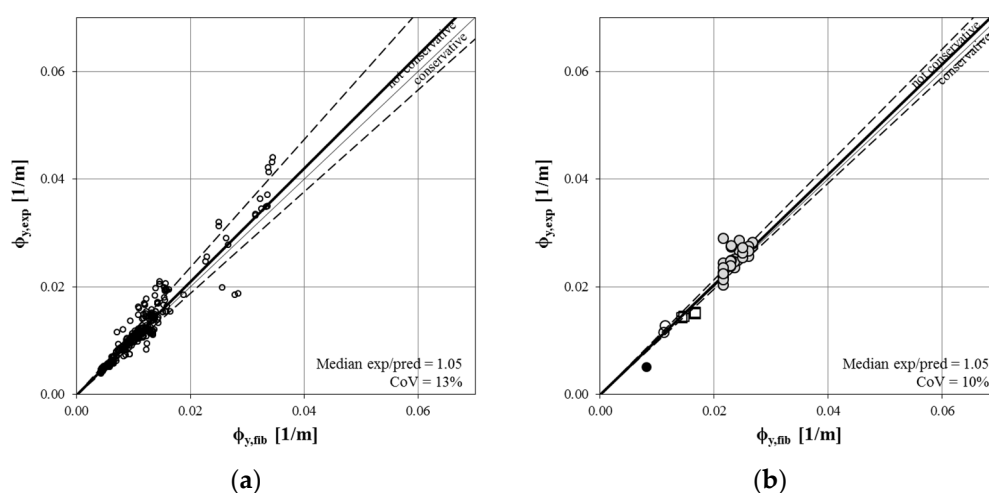
Figure 8. Comparison of experimental and predicted ϕ_y for (**a**) DB and (**b**) WB of the database; in (**b**), similar symbols are used for each experimental source.

Conversely, quite poorer fitting is shown for ϕ_u. If stirrups with 90° closed hooks are assumed to not provide any confinement at all, corresponding beams show large underestimation of ϕ_u than the rest (see Figure 9a). In fact, this assumption is intended to

be feasible for design purposes, given that it furnishes conservative results. However, the real influence of hooks on stress–strain models is not clearly quantified; a modification of Mander's confinement model for columns with 90° closed hooks is proposed in [32]. If full confinement is assumed for beams with 90° closed hooks in which some confinement would be expected if 135° closed hooks were used (i.e., in beams with $\alpha > 0$), the error reduces largely (see Figure 9b), even when only 56 out of 277 beams belong to this group. Regarding the application of fundamental approaches for the estimation of θ_u (based on ϕ values), the last assumption is adopted herein. For empirical approaches, it is not relevant because the influence of confinement is significantly lower (see Section 1) and also because, in the particular case of the present database, beams with 90° closed hooks show lower density of stirrups, thus providing low values of α.
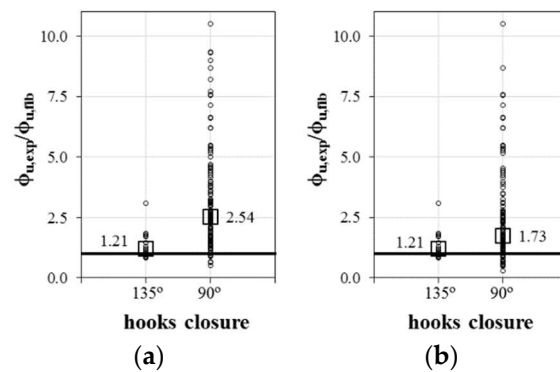

(a) (b)

Figure 9. Comparison of experimental and predicted ϕ_u for all the DB of the database, considering 90°-hook closed stirrups as (**a**) ineffective and (**b**) fully effective aimed at confining of concrete core; mean values with square marker.

In Figure 10, experimental and predicted ϕ_u are compared. High underestimation and very large dispersion of results are shown especially for DB. It is worth noting that the adopted confinement model has been obtained as a regression of the whole original database, including columns. It should be necessary to apply the same procedure to the columns belonging to the database in order to know whether the generalised bias in beams is balanced by columns or not. In the last case, the difference of results may rely on the different approach on curvature calculation, even when similar models are adopted. It emphasises the higher sensitivity of fundamental procedures for θ with respect to empirical ones regarding steel type or seismic detailing.
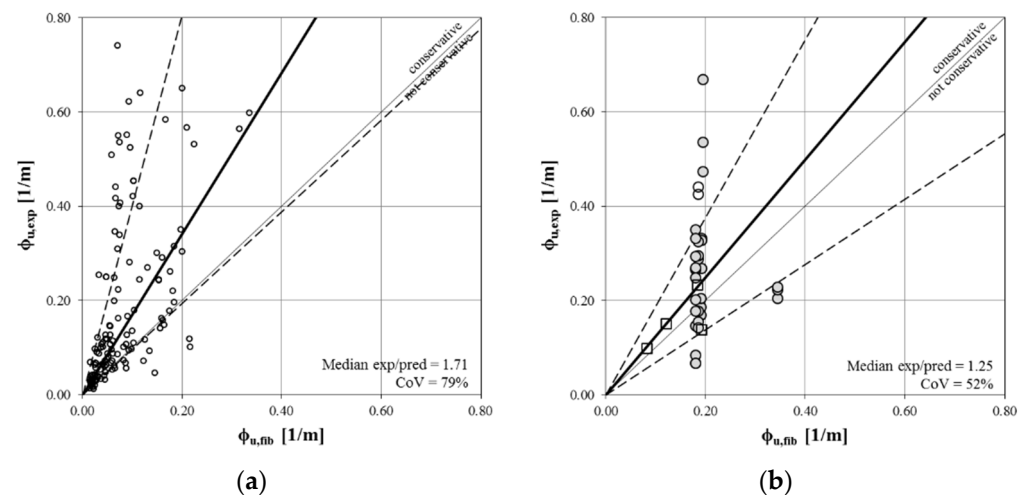

(a) (b)

Figure 10. Comparison of experimental and predicted ϕ_u for (**a**) DB and (**b**) WB of the database, considering full confinement in beams with 90°-hook closed stirrups.

3.2. Chord Rotations

Regarding θ, different formulations proposed in [23,25,26] are applied separately to the disaggregated sub-databases DB and WB. In Equations C1 to C8 of Appendix B, all the expressions are presented in a homogenised form. In the following, subscripts "*emp*" and "*fun*" denote empirical and fundamental approaches, respectively. Formulations from ASCE (Equation (5) and Table 1) are also performed.

Median values and dispersion magnitudes of all the cases are shown in Table 3. As expected, ASCE formulations show much poorer fitting than the rest, as they largely underestimate chord rotations. Both P&F and B&F approaches slightly underestimate θ_y both for DB and WB, which is not conservative; conversely, they underestimate θ_u for DB (which is conservative) and overestimate θ_u for WB (not conservative). Empirical approaches show better fitting than fundamental ones: in the first case, median experimental-to-predicted ratios are always within ± 20% with respect to perfect fitting, while in the second case, it can reach 100%, due to the high uncertainty regarding the calculation of curvatures.

Table 3. Fitting of different expressions for predicted θ with respect to experimental disaggregated data.

Experimental-to-Predicted Ratio		Expression for Prediction	DB		WB	
			Median	CoV	Median	CoV
$\theta_{y,exp}/$	$/\theta_{y,P\&F}$	Equation (A18)	1.02	35%	1.06	21%
	$/\theta_{y,B\&F}$	Equation (A19)	1.07	34%	1.14	21%
	$/\theta_{y,ASCE}$	Equation (5)	1.30	68%	4.24	44%
$\theta_{u,exp}/$	$/\theta_{u,P\&F,emp1}$	Equation (A20)	1.14	47%	0.88	40%
	$/\theta_{u,P\&F,emp2}$	Equation (A21)	1.00	52%	0.95	44%
	$/\theta_{u,B\&F,emp1}$	Equation (A22)	1.19	46%	0.84	38%
	$/\theta_{u,B\&F,emp2}$	Equation (A23)	1.21	47%	0.90	37%
	$/\theta_{u,B\&F,fun}$	Equations (A24) and (A25)	2.06	68%	0.88	46%
	$/\theta_{u,ASCE}$	Table 1 + Equation (5)	2.19	74%	1.60	51%

In general, the P&F model shows better fitting than B&F, as the original database from which it comes out as a regression is more similar to the sub-databases used herein (e.g., it does not include sections different from rectangular shape). However, the present work focuses mainly on B&F because it is the basis of current EC8-3 formulations. Except for the fundamental approach, dispersion levels in all the cases are rather similar to those observed in the original works.

In Figure 11, experimental and predicted θ_y for the B&F model are compared. Larger underestimation but lower dispersion is shown for WB rather than for DB. The median experimental-to-predicted ratio for all the beams (DB + WB) is 1.11 if WB values are weighted in order to provide a similar contribution to the median despite their lower number of tests, or 1.08 otherwise. No particular bias is shown for the different sub-groups (i.e., steel class, type of loading, possibility of slippage, or hook closure angle).

Regarding θ_u, in Figure 12, experimental and predicted values for the B&F first empirical model are compared. Almost exactly symmetric bias is shown for DB and WB: median experimental-to-predicted ratios for both cases are inverse (1.19 for DB and 0.84 for WB); better fitting is shown by P&F's second model (1.00 and 0.95, respectively). If both sub-databases are merged, weighted median values of 0.94 are obtained, which is not conservative. It is worth noting that the bias is more important for the sub-groups that likely represent current seismic-designed buildings: hot-rolled ductile steel, cyclic loading, slippage of longitudinal reinforcement, and seismic detailing of stirrup hooks (see Figure 13). In fact, EC8-3 assumes by default the formulations corresponding to cyclic loading and slippage.
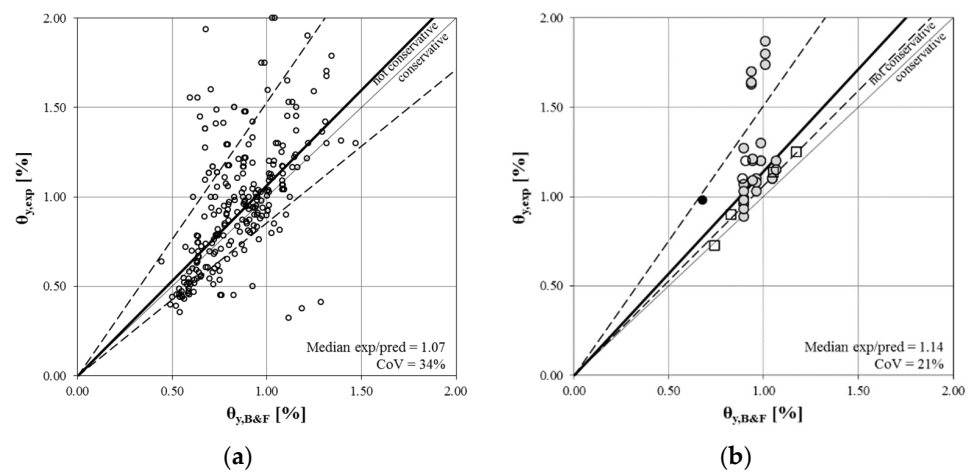
Figure 11. Comparison of experimental and predicted θ_y according to [25] for (**a**) DB and (**b**) WB of the database; mean values with square marker.
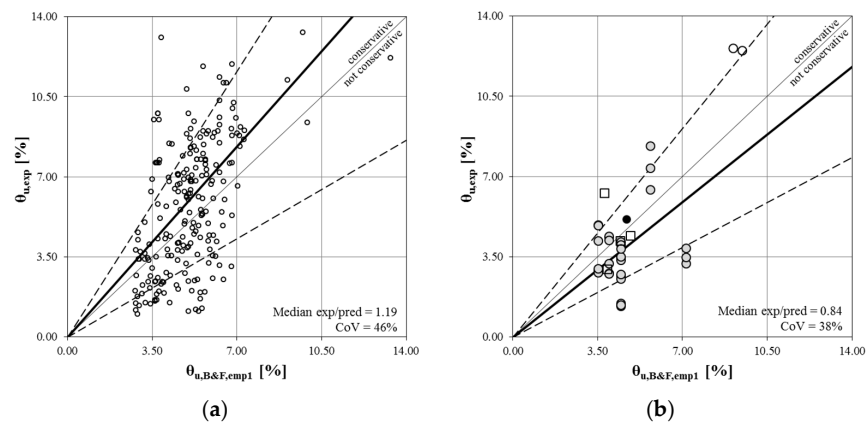

Figure 12. Comparison of experimental and predicted θ_u according to the first empirical formulation in [26] for (**a**) DB and (**b**) WB of the database.
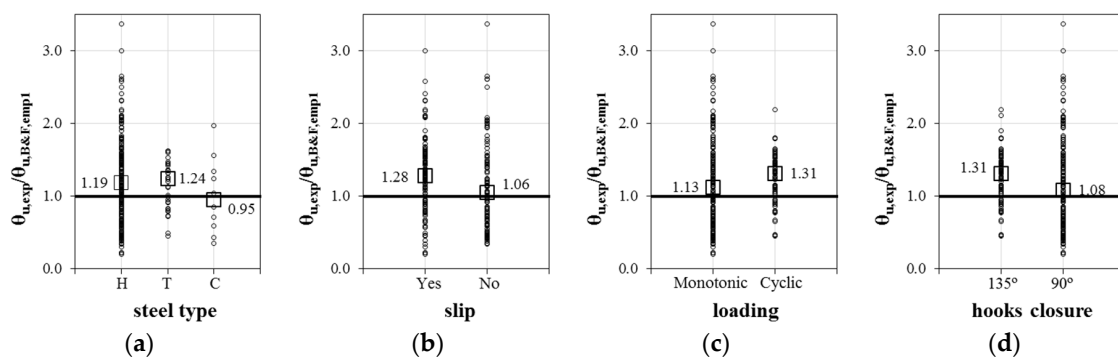
Figure 13. Experimental-to-predicted ratios of θ_u according to the empirical formulation in [26] for DB, disaggregated for different cases: (**a**) steel type (H: hot-rolled; T: tempcore; C: cold worked); (**b**) slippage; (**c**) type of loading; and (**d**) hook closure beams.

The B&F's fundamental approach (see Figure 14) shows rather similar underestimation of θ_u for WB (median values of 0.88), but the overestimation for DB is huge (2.06), even when curvatures corresponding to perfect confinement also for 90° closed hooks are assumed. This may suggest that values of L_{pl} are highly underestimated for DB and overestimated for WB, even when they are higher for DB rather than for WB as they increase with h_b. Conversely to the empirical approach, experimental-to-predicted ratios do not show

significant bias when disaggregated for the different sub-groups (i.e., loading, steel, etc.). For the merge of sub-databases, a weighted median ratio of 1.16 is shown.

Figure 14. Comparison of experimental and predicted θ_u according to the fundamental formulation in [26] for (**a**) DB and (**b**) WB of the database.
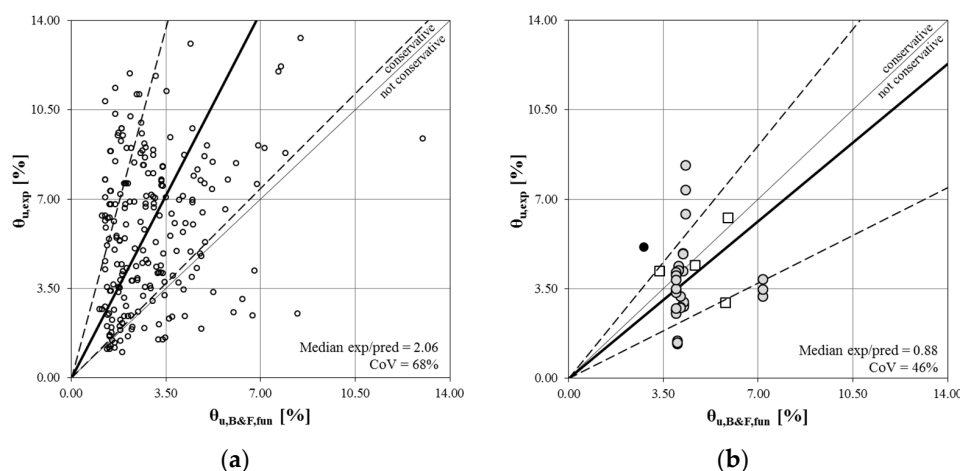
Undoubtedly, the reliability of the results obtained in this section may be under discussion, considering the limited number of tests belonging to sub-database WB and also the reduced variability of cases. However, in almost all the cases, the median experimental-to-predicted ratios for the merge of both sub-databases DB and WB are roughly near to 1.0, which means that those few results of WB provide a kind of balance to DB ones, whose reliability is higher. Additionally, lower bias is observed for WB than for DB.

4. Proposal of Corrected Expressions

In the previous section, the application of formulations on the basis of the current procedure in EC8-3 separately to DB and WB shows that experimental θ_u is lower than that predicted for WB and higher than that predicted for DB, while experimental θ_y is slightly higher than that predicted mainly for WB.

In this section, some corrections for the formulations of [25,26] are proposed, in order to reduce the bias and thus increase the robustness of the deformation model against cross-sectional shape variations. This proposal should be understood purely as an available simple alternative for the assessment of buildings with WB, or to be used for compared analysis of WB and DB, for instance. The current approach in EC8-3 makes no explicit distinction between columns and beams aimed at the estimation of θ. Hence, any alternative set of formulations able to account for the cross-sectional aspect ratio should also be checked for columns, which is not possible to be carried out with the existing database because cross-sectional orientation is always similar in most cases.

The proposals are intended as slight modifications within the framework of the formulations, which is not altered. In some cases, independent contribution factors are added, while in other cases, new parameters are placed within other contributions. In all the cases, corrections are carried out only on the part of the body of formulations which is purely empirical, aimed at best-fitting.

However, some premises according to previous results could be followed aimed at the definition of the correction parameters. Firstly, they must refer to the geometry of the section (h_b and/or b_w), which are also responsible for different performances of DB and WB regarding curvatures (see Section 1). In order to be consistent with the disaggregation of the original database that allowed determining the bias (see Section 2), maybe the most feasible factor to be used would be the cross-sectional aspect ratio (h_b/b_w), which is on the basis of the definition of DB and WB consistent with a "corner" value of 1.0. Still, all

the expressions already contain terms depending on h_b; thus, different attempts aimed at avoiding such duplicity are carried out.

Regarding θ_u, the influence of aspect ratio can be intended as being divided into two contributions, as it influences both ϕ and L_{pl} (see Section 1). The fundamental approach already takes into account the important influence on ϕ; thus, any further influence of aspect ratio should concern only L_{pl}, in such a way that it increases for DB and decreases for WB. Conversely, in an empirical approach, both implicit contributions of aspect ratio on ϕ and L_{pl} are concentrated mainly in the factor $h_b^{-0.35}$ and to a lesser extent on the confinement factor $25^{\alpha \cdot \omega w}$; the latter is not modified in the proposal.

Firstly, the form of the expressions is chosen. Four different forms for the corrected empirical formulations for θ_u are proposed; they are shown in Equations (6)–(9), in which parameters C_1 and C_2 are defined in each formula for best fitting, i.e., experimental-to-predicted ratio equal to 1.0 and the lowest dispersion. Aimed at easing the awareness of the differences between formulations, some of their members are condensed with respect to the original expression in Equation (A22) (see Appendix B): $a = a_{st}[1 - a_{old} \cdot a_{cy}(1 + 0.25a_{pl})/6]$ $(1 - 0.43a_{cy})(1 + a_{sl}/2)$; $k_\alpha = 25^{\alpha \cdot \omega w}$; $k_\rho = 1.25^{100\rho d}$; $k_\omega = (\max\{0.01; \omega\}/\max\{0.01; \omega'\} \cdot f_c)^{0.225}$.

$$\theta_{u,emp1,\text{mod1}} = a \cdot k_\omega \cdot k_\alpha \cdot k_{\rho d} \left(\min\left\{ \frac{L_V}{h_b}; 9 \right\} \right)^{0.35} \left(\frac{h_b}{b_w} \right)^{C_1} \tag{6}$$

$$\theta_{u,emp1,\text{mod2}} = a \cdot k_\alpha \cdot k_{\rho d} \cdot k_\omega \left(\min\left\{ \frac{L_V}{h_b}; 9 \right\} \right)^{0.35} \left(\frac{C_2}{b_w} \right)^{C_1} \tag{7}$$

$$\theta_{u,emp1,\text{mod3}} = a \cdot k_\alpha \cdot k_{\rho d} \cdot k_\omega \left(\min\left\{ \frac{L_V}{\sqrt{b_w h_b}}; 9 \right\} \right)^{C_1} \tag{8}$$

$$\theta_{u,emp1,\text{mod4}} = a \cdot k_\alpha \cdot k_{\rho d} \cdot k_\omega \left(\min\left\{ \frac{L_V}{\sqrt[3]{b_w h_b{}^2}}; 9 \right\} \right)^{C_1} \tag{9}$$

The first proposal is to multiply the original formulation by a power of aspect ratio (Equation (6)), which increases θ_u of DB and decreases θ_u of WB. In order to avoid the duplicity of terms depending on h_b, a second option, based on a factor only depending on b_w, is proposed (Equation (7)). However, this option needs to be given a "corner" value for b_w in order to define the threshold for the increase or decrease in θ_u, which is actually kind of a definition of DB and WB regarding only b_w, being in some cases insufficient. On the other hand, the third and fourth options are essentially based on the combined influence of h_b and b_w on relative ultimate curvatures (see Section 1). In the third option (Equation (8)), the original denominator h_b is replaced by the geometric mean of h_b and b_w (in order to keep the dimensionless character of the shear span). In the fourth option (Equation (9)), a similar approach is proposed, but more importance is given to h_b.

Regarding the fundamental approach for θ_u, corrections should be performed on the value of L_{pl} (Equation (A25), see Appendix B). The theoretical relation between L_{pl} and cross-sectional geometry (h_b and b_w) is not clearly defined in the literature. The expression proposed in [27] considers L_{pl} as a constant ratio (8%) of L_V plus an increment due to slippage, thus independent of the cross-sectional geometry. In [23], a similar form of the expression is assumed. Conversely, in [26], a term depending on h_b is added, whose weight may be comparable to that of L_V. In any of those approaches b_w is proposed as a relevant variable.

Two options for modifying Equation (A25) are proposed, in order to obtain larger values for DB and shorter ones for WB. Parameters C_1 to C_4 are analogously defined in each formula for best fitting with experimental data. In the first one (Equation (10)), h_b is multiplied by the aspect ratio; conversely, in the second proposal (Equation (11)), the higher difference between DB and WB is intended to be reached by emphasising the relative contribution of h_b at the expense of the term dependent on L_V, without any contribution of b_w. However, several attempts aimed at conducting an optimisation of the last expression

show values of $C_3 = C_4 = 0$ and still very large dispersion. Hence, only the first option (Equation (10)) is developed.

$$L_{pl,\text{mod}1} = \begin{cases} 0.04\min\{L_V; 9h_b\} + C_1 \cdot h_b\left(\dfrac{h_b}{b_w}\right) \text{ (monotonic)} \\ 0.0\widehat{6}\min\{L_V; 9h_b\} + C_2 \cdot h_b\left(\dfrac{h_b}{b_w}\right) \text{ (cyclic, seismic design)} \end{cases} \quad (10)$$

$$L_{pl,\text{mod}2} = \begin{cases} C_3 \cdot \min\{L_V; 9h_b\} + C_1 \cdot h_b \text{ (monotonic)} \\ C_4 \cdot \min\{L_V; 9h_b\} + C_2 \cdot h_b \text{ (cyclic, seismic design)} \end{cases} \quad (11)$$

Finally, a proposal for a correction of the formulation for θ_y (Equation (12)) is also made. Only the shear contribution (last term) should be modified. Analogously to Equation (8), h_b is replaced by the geometric mean of h_b and b_w.

$$\theta_{y,\text{mod}} = \phi_y\left(\frac{L_V + a_v z}{3} + a_{sl} \cdot 0.125 d_{bL}\frac{f_y}{\sqrt{f_c}}\right) + 0.0014\left(1 + C_1\frac{\sqrt{b_w h_b}}{L_V}\right) \quad (12)$$

Proposed parameters for all the formulations are shown in Table 4. Rather satisfactory solutions are found when compared to Table 3: similar dispersion levels to the original formulations are shown, except for the corrected fundamental approach (Equation (10)). Perfect fitting is shown for corrected θ_y (see Figure 15) and for the second option of corrected θ_u (see Figure 16). In the rest of the expressions, the bias of results is rather symmetric and much more reduced than in the original ones: mean ratios are approximately within ±5% with respect to perfect fitting, except for the fourth option for corrected θ_u in DB (+14%).

Table 4. Selected values of parameters providing best fitting of proposed corrected expressions for θ within merged experimental database.

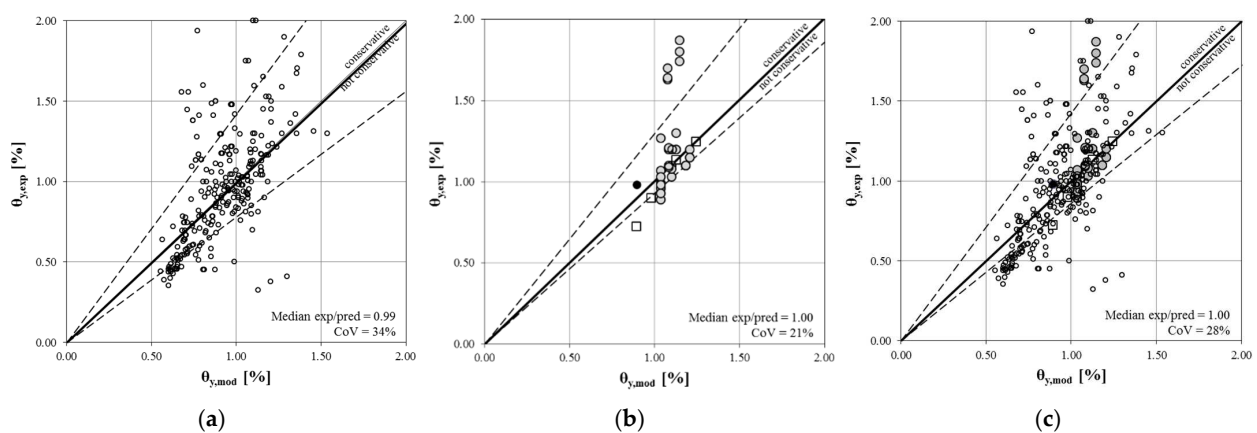| Corrected Expression	Equation	Proposed Parameters		Experimental-to-Predicted Ratios					
				All Cases		DB		WB	
		C_1	C_2	Median	CoV	Median	CoV	Median	CoV
$\theta_{y,mod}$	(12)	4.64	-	1.00	28%	0.99	34%	1.00	21%
$\theta_{u,emp1,mod1}$	(6)	0.20	-	1.00	43%	1.04	48%	0.98	38%
$\theta_{u,emp1,mod2}$	(7)	0.40	262 mm	1.00	45%	1.00	47%	1.00	43%
$\theta_{u,emp1,mod3}$	(8)	0.35	-	1.00	43%	1.06	47%	0.96	38%
$\theta_{u,emp1,mod4}$	(9)	0.33	-	1.00	43%	1.14	47%	0.95	38%

Figure 15. Comparison of experimental and predicted θ_y according to the proposed correction (Equation (12)) to the formulation in [25] for (**a**) DB, (**b**) WB, and (**c**) the weighted merge of both sub-sets of the experimental database.
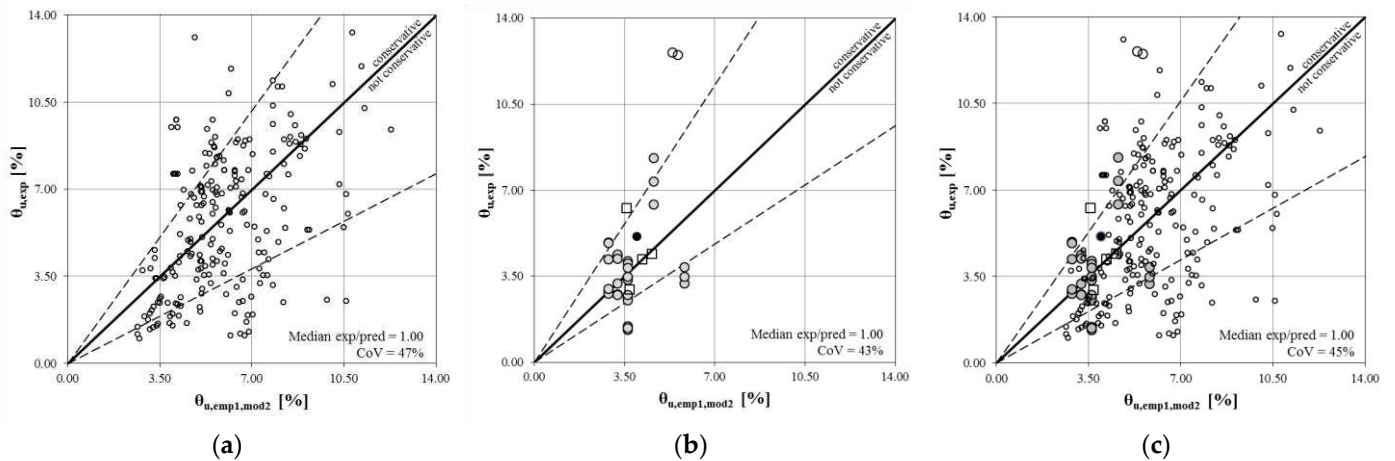
Figure 16. Comparison of experimental and predicted θ_u according to the second proposed correction (Equation (7)) to the formulation in [25] for (**a**) DB, (**b**) WB, and (**c**) the weighted merge of both sub-sets of the experimental database.

Regarding bias corresponding to different disaggregations of sub-databases (steel type, slippage, loading type, and hook closure; see Table 5), corrected θ_y values show quite good balance, in accordance with the reduced global CoV. The first two proposals for corrected empirical θ_u also show rather good balance, but quite large bias is shown by the third and fourth proposals and especially by the fundamental approach, whose reliability is actually lower.

Table 5. Disaggregated experimental-to-predicted ratios for proposed corrected expressions on different subsets of DB from the experimental database.

Corrected Expression	Median Experimental-to-Predicted Ratios								
	Steel Type			**Slippage**		**Loading**		**Hooks**	
	Hot-Rolled	Tempcore	Cold	Yes	No	Monotonic	Cyclic	135°	90°
$\theta_{y,mod}$	1.00	0.94	1.01	1.01	0.98	0.97	1.06	1.05	0.97
$\theta_{u,emp1,mod1}$	1.03	1.15	0.83	1.15	0.89	0.93	1.18	1.17	0.92
$\theta_{u,emp1,mod2}$	0.99	1.08	0.79	1.13	0.89	0.91	1.19	1.18	0.90
$\theta_{u,emp1,mod3}$	1.05	1.16	0.84	1.17	0.92	0.95	1.19	1.19	0.94
$\theta_{u,emp1,mod4}$	1.13	1.22	0.91	1.23	1.00	1.02	1.26	1.25	1.01

Finally, some of those proposals are applied to the set of DB and WB analysed in Section 1 (see Table 2), in order to obtain more realistic values of deformations and thus a more representative comparison of ductilities between both types. In most cases, it is possible to apply the same corrections, previously proposed for expressions in [25,26], to the EC8-3 formulations (Equations (1) and (4)), because they correspond to a particular case of those ones. The last is not possible only for the fundamental approach, given that the two approaches show different confinement models, different contributions of fixed-end rotation at ultimate deformation, and also different expressions of L_{pl}. Hence, the final proposal of corrected expressions for EC8-3 is presented in Equation (13) for θ_y and Equations (14) and (15) for θ_u, since they show better fitting than the rest.

$$\theta_{y,EC8,\text{mod}} = \phi_y \left(\frac{L_V + a_v z}{3} + 0.13 d_{bL} \frac{f_y}{\sqrt{f_c}} \right) + 0.0013 \left(1 + 4.64 \frac{\sqrt{b_w h_b}}{L_V} \right) \quad (13)$$

$$\theta_{u,EC8,emp,\text{mod}1} = 0.016 \left(\frac{\max\{0.01; \omega'\}}{\max\{0.01; \omega\}} f_c \right)^{0.225} \left(\frac{L_V}{h_b} \right)^{0.35} \left(\frac{h_b}{b_w} \right)^{0.2} \cdot 25^{\alpha\omega_w} \cdot 1.25^{100\rho_d} \quad (14)$$

$$\theta_{u,EC8,emp,mod2} = 0.016 \left(\frac{\max\{0.01;\omega'\}}{\max\{0.01;\omega\}} f_c \right)^{0.225} \left(\frac{L_V}{h_b} \right)^{0.35} \left(\frac{262\,mm}{b_w} \right)^{0.4} \cdot 25^{\alpha\omega_w} \cdot 1.25^{100\rho_d} \qquad (15)$$

The results are shown in Figure 17 for Equations (13) and (14). Equation (15) causes a reduction in values also for DB, given that those beams have b_w = 300 mm, which is common for this kind of beam but higher than the "corner value" of 262 mm. In fact, such a value is obtained for best fitting with the sub-database of DB, which contains a high number of scaled specimens (255 out of 272 with b_w < 262 mm). This is not an issue for the original expressions and for the rest of the proposed corrected formulations, in which cross-section geometry measures are always rated to L_V. Hence, Equation (14) may be more robust than Equation (15).
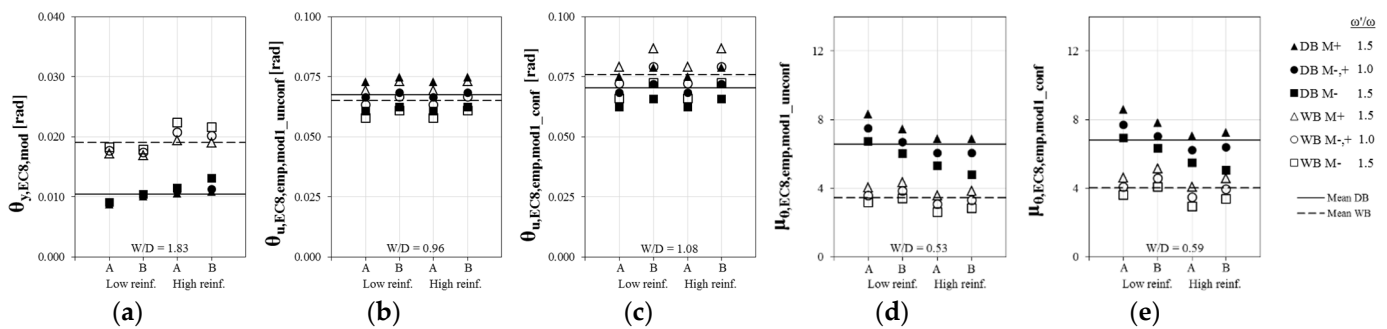

Figure 17. (**a**) θ_y; (**b**) θ_u for unconfined case; (**c**) θ_u for confined case; (**d**) μ_θ for unconfined case; and (**e**) μ_θ for confined case in all the beams of the parametric set according to the first proposal for corrected EC8-3 formulations.

Mean θ_u (Figure 17a,b) shows an increase of 13% for DB and a decrease of 12% for WB, which are slightly lower than the bias of median experimental-to-predicted ratios for the corresponding sub-databases (+19% for DB and −16% for WB, see Table 3 and Figure 12). These modifications result in rather similar θ_u values for WB and DB for both confined and unconfined cases ($\theta_{u,W/D,unconf}$ = 0.96 and $\theta_{u,W/D,conf}$ = 1.08, on average). On the other hand, equivalent implicit L_{pl} according to these values becomes always lower for WB than for DB ($L_{pl,et,W/D}$ = 0.95 and 0.45 for unconfined and confined sections, respectively), which is consistent with the explicit expression of L_{pl} in the fundamental approach.

Consequently, according to the corrected model, even lower local ductilities are expected for WB than for DB ($\mu_{\theta,W/D}$ = 0.53 and 0.59 for unconfined and confined cases instead of 0.67 and 0.75, respectively; see Figure 17c,d).

Nevertheless, it cannot be the cause of the imposition of lower behaviour factors (*q*) for WBF in past codes, because even the original deformation models are more recent than those prescriptions. Moreover, such a lack of local ductility of WB with respect to DB should not become a reason for any further prescription in current seismic codes regarding a limit of *q* for wide-beam frames (WBF). In fact, the local ductility of beams appears to be only one of the parameters governing the global capacity of WBF when the damage limitation limit state is the most critical condition of design, as in most EC8-designed buildings [7,8]. First of all, local ductility of columns is able to balance the global ductility of the frame; the rest of the modern code's provisions result in favourable design results for WBF rather than for DBF (e.g., larger L_V of first storey columns or higher stiffness of joints).

5. Conclusions

The current model proposed by Eurocode 8 part 3 predicts that the chord rotation ductility of wide beams is lower than in conventional deep beams despite the similar curvature ductilities, due to lower plastic hinge lengths in WB.

However, those formulations have been proved to show some bias when applied separately to the wide and deep beams belonging to the original database from which that model was derived. Predicted chord rotations compared with experimental values

are consistently conservative for DB and not conservative for WB, especially at ultimate deformation. Thus, the current model is still underestimating the difference in plastic hinge between both beam types of beams: they should be even larger for DB.

Therefore, some feasible correction factors have been proposed in order to improve the prediction capacity of the current model, for both the pure empirical and fundamental formulations. Factors considering cross-sectional geometry are included in the original formulations, and parameters aimed at best fitting with experimental data are searched. Rather satisfactory solutions with similar dispersion and no bias have been obtained; thus, the correction may increase the robustness of the model against cross-sectional shape variability. Given the reduced amount of WB in the original database, further experimental research would be required in order to increase the reliability of the corrections.

Author Contributions: Conceptualisation, methodology, validation, writing, F.G.-M.; Data curation, A.P.-G. All authors have read and agreed to the published version of the manuscript.

Data Availability Statement: Not applicable.

Conflicts of Interest: The paper is based on a short communication presented by the authors at the 16th World Conference on Earthquake Engineering, WCEE, Santiago, Chile, 9–13 January 2017.

Nomenclature

$[]_{emp}$	Empirical value of any parameter []
$[]_{fun}$	Fundamental value of any parameter []
$[]_{W/D}$	Ratios between values corresponding to WB and DB for any parameter []
a_{cy}	Zero-one parameter for cyclic loading
a_{old}	Zero-one parameter for 90° closed hooks
a_{pl}	Zero-one parameter for plain bars and slippage
A_{s1}	Tensioned reinforcement area
A_{s2}	Compressed reinforcement area
ASCE	ASCE-SEI/41-06
a_{sl}	Parameter for steel class
a_v	Zero-one parameter for pre-yielding shear concrete cracking
B&F	Biskinis and Fardis
b_w	Cross-section width
C	Optimisation factors
c_n	Concrete cover
CoV	Coefficient of variation
d	Effective depth
d'	Distance from extreme fibres to the axe of reinforcement
DB	Deep beams
DBF	Deep-beam frames
d_{bL}	Mean diameter of longitudinal reinforcement
d_{bt}	Mean diameter of transverse reinforcement
DCH	High ductility class
EC8-1	Eurocode 8 part 1
EC8-1	Eurocode 8 part 3
$E_{sec}{}'$	Equivalent secant Young's modulus corresponding to triangular stress distribution
f_c	Resistance of concrete
F_c	Compression force in concrete
f_u	Ultimate steel strength
f_y	Yielding steel strength
h_b	Cross-section height
K_{sec}	Secant-to-yielding member stiffness
L_{pl}	Plastic hinge length

$L_{pl,eq}$	Equivalent implicit value of plastic hinge length
L_V	Shear span
M_u	Ultimate bending moment
M_y	Yielding bending moment
P&F	Panagiotakos and Fardis
q	Behaviour factor
RC	Reinforced concrete
s_t	Stirrup spacing
U_{s1}	Tension force in reinforcement
V_{pl}	Maximum shear corresponding to the attainment of moment resistances
V_s	Stirrup shear strength contribution
WB	Wide beams
WBF	Wide-beam frames
x	Neutral axis depth
z	Internal lever arm
α	Confinement effectiveness factor
α_{cy}	Parameter for type of loading
$\alpha_{st,cyc}$	Parameter for steel class in cyclic tests
$\alpha_{st,mon}$	Parameter for steel class in monotonic tests
ε_c	Concrete maximum strain
ε_{su}	Steel ultimate strain
θ_{pl}	Plastic chord rotation
θ_u	Ultimate chord rotation
θ_y	Yielding chord rotation
μ_θ	Chord rotation ductility of the member
μ_ϕ	Curvature ductility of the cross-section
ρ_{bal}	Reinforcement ratio for balanced strain conditions
ρ_d	Diagonal reinforcement ratio
ρ_w	Transverse reinforcement ratio
σ_c	Concrete maximum stress
ϕ_u	Ultimate curvature
$\phi_{u,conf}$	Ultimate curvature with confined concrete core
$\phi_{u,unconf}$	Ultimate curvature with unconfined concrete core
ϕ_y	Yielding curvature
$\phi_{y,exp}$	Indirect curvature values obtained from experimental values of yielding moment
ω	Bottom mechanical reinforcement ratio
ω'	Top longitudinal mechanical reinforcement ratio
ω_{tot}	Total longitudinal mechanical reinforcement ratio
ω_w	Transverse mechanical reinforcement ratio

Appendix A. Fundamental Comparison between Wide and Deep Beams Regarding Cross-Sectional and Member Ductilities

Cross-sectional ductility comparison is carried out by operating two generic beams (one DB and one WB, $h_{b,W/D} \leq 1$) with similar M_y, (ω'/ω) and L_V. M_y is approximately proportional to d, given that similar z values are expected both for DB and WB because $b_{w,W/D} \geq 1$. Considering that $M_y = A_{s1} \cdot z$, then $A_{s1,W/D} \approx 1/d_{W/D}$.

Firstly, regarding $\mu_{\phi,W/D}$, it can be assumed that ϕ_y is attained by yielding of tensioned reinforcement, and the distribution of tensions in concrete can be considered almost triangular; thus, $\sigma_c = E_{sec}' \cdot \varepsilon_c$, being σ_c and ε_c the concrete maximum stress and strain (at top fibre in positive bending) and E_{sec}' the equivalent secant Young's modulus corresponding to triangular stress distribution. In the first step, it is considered that $\omega' = 0$. Hence, the compression force in concrete $F_c = 0.5 \cdot x \cdot b_w \cdot E_{sec}' \cdot \varepsilon_c$ must be equal to the tension force in reinforcement $U_{s1} = A_{s1} \cdot f_y$. Making $F_c = U_{s1}$, and considering that $\phi_y = \varepsilon_c/x$, Equation (A1) is obtained. Consequently, $\phi_{y,W/D}$ can be expressed as in Equation (A2)

by making $A_{s1,W/D} = 1/d_{W/D}$. On the other hand, if $\phi_{y,W/D} = \varepsilon_{c,W/D}/x_{W/D}$ is replaced in Equation (A2), then Equation (A3) is obtained.

$$\phi_y = \frac{A_{s1}f_y}{0.5x^2 b_w E_{\text{sec}}\prime} \tag{A1}$$

$$\phi_{y,W/D} = \frac{1}{b_{w,W/D} \cdot d_{W/D} \cdot x_{W/D}^2} \tag{A2}$$

$$\varepsilon_{c,W/D} = \frac{1}{b_{w,W/D} \cdot d_{W/D} \cdot x_{W/D}} \tag{A3}$$

By means of geometric compatibility, $\phi_y = \varepsilon_{sy}/(d-x)$; thus, $x = \varepsilon_{c}/\varepsilon_{sy}(d-x)$ (see Figure 1). Considering that $\varepsilon_{sy,W/D} = 1$ and that $(d-x)_{W/D} \approx d_{W/D}$ (x negligible compared to ratios of d), then Equation (A4) is obtained. Subsequently, if Equation (A3) is replaced by Equation (A4), then Equation (A5) is obtained, which shows that WB may present shorter x than DB due to their larger width. Finally, if Equation (A5) is replaced by Equation (A2), then the approximated expression for $\phi_{y,W/D}$, depending only on the relative geometry between WB and DB, is provided in Equation (A6). The last expression can be considered as representative also when $\omega' \neq 0$, because top reinforcement may be subjected to stresses quite lower than f_y for amounts of ω_{tot} corresponding to design in DCH. Even when important stresses are required, they may be rather similar for WB and DB given that steel yielding occurs pre-emptively and that x cannot be so large for design in DCH; thus, d' may be close to the fibre corresponding to the crossing point between strain plains of WB and DB.

$$x_{W/D} = \varepsilon_{c,W/D} \cdot d_{W/D} \tag{A4}$$

$$x_{W/D}^2 = 1/b_{w,W/D} \tag{A5}$$

$$\phi_{y,W/D} = 1/d_{W/D} \tag{A6}$$

Hence, relative secant-to-yielding stiffness between WB and DB seems to be inversely proportional to the section depth, which means that WBs are relatively more rigid at yielding than at initial uncracked state when compared to DBs in most cases.

For the evaluation of $\phi_{u,W/D}$, similar reasoning can be made. In this case, constant concrete stress distribution (i.e., rectangular stress block) is considered (see Figure 1). If confinement is not taken into account, the ultimate deformation state in the section may correspond to failure of concrete in compression; thus, $F_c = 0.8 \cdot x \cdot b_w \cdot f_c$. Analogously to the previous development, $x_{W/D,unconf} = A_{s1,W/D}/b_{W/D} = 1/b_{W/D}$, and consequently, $\phi_{u,W/D,unconf}$ is obtained as in Equation (A7), and corresponding ductility $\mu_{\phi,W/D,unconf}$ is expressed as in Equation (A8).

$$\phi_{u,W/D,unconf} = b_{W/D} \cdot d_{W/D} \tag{A7}$$

$$\mu_{\phi,W/D,unconf} = b_{W/D} \cdot d_{W/D}^2 \tag{A8}$$

Hence, if their cross-sectional areas are rather similar, WB and DB are expected to show similar ultimate curvatures, and consequently, the lack of ductility of WB with respect to DB is proportional to their effective depths.

However, design in DCH provides an important confinement of the concrete core, so a different reasoning must be developed. In this case, the ultimate deformation state in the section may correspond to excessive deformation of steel in tension [6]. Therefore, $\phi_{u,conf} = \varepsilon_{su}/(d-x)$, and consequently, $\phi_{u,W/D,conf} = \varepsilon_{su,W/D}/(d-x)_{W/D}$ (see Figure 1). Considering that $\varepsilon_{su,W/D} = 1$ and also that $(d-x)_{W/D} \approx d_{W/D}$, then $\phi_{u,W/D,conf}$ can be expressed as in Equation (A9), which is similar to the relationship between yielding curvatures, thus leading to similar curvature ductilities for both types of beams (Equation (A10)).

$$\phi_{u,W/D,conf} = 1/d_{W/D} \tag{A9}$$

$$\mu_{\phi,W/D,conf} = 1 \tag{A10}$$

For the sake of comparison of member ductilities, considerations are elaborated within the framework of EC8-3 and ASCE methods.

For ASCE, $\theta_{y,W/D} = b_{w,W/D} \cdot h_{b,W/D}{}^3$, as it only depends on gross stiffness. Within the EC8-3 approach, $\theta_{y,W/D}$ may be a bit lower than $\phi_{y,W/D}$ because the contribution of shear deformation increases with depth. Thus, likely, $\theta_{y,W/D}$ can be expressed as in Equation (A11) if $\phi_{y,W/D}$ is replaced as in Equation (A6). Regarding the fundamental approach for ultimate deformations, $\theta_{u,W/D}$ could be estimated as $L_{pl,W/D} \cdot \phi_{u,W/D}$ (i.e., proportional to ultimate curvatures through plastic hinge length) if L_{pl} is considered as negligible with respect to L_V and especially if yielding deformations are assumed to be negligible with respect to ultimate ones when compared between WB and DB ($\theta_{pl,W/D} \approx \theta_{u,W/D}$ and $\phi_{pl,W/D} \approx \phi_{u,W/D}$). The last may be more likely to occur for confined beams, in which ultimate deformations are much larger [23]. Then, taking into account also the result in Equation (A11), $\theta_{u,W/D} \geq L_{pl,W/D} \cdot \phi_{u,W/D}$. Regarding L_{pl}, proposed expressions increase with h_b; thus, $L_{pl,W/D} \leq 1$. Hence, likely, $\theta_{u,W/D}$ could be approximated as in Equations (A12) and (A13) for unconfined and confined cases, respectively, replacing $\phi_{u,W/D}$ by Equations (A7) and (A8), respectively. Subsequent ductility ratios are shown in Equations (A14) and (A15) for unconfined and confined cases, respectively, which are similar to those corresponding to curvatures.

$$\theta_{y,W/D,EC8} \leq 1/d_{W/D} \tag{A11}$$

$$\theta_{u,W/D,EC8\_fun,unconf} \leq b_{W/D} \cdot d_{W/D} \tag{A12}$$

$$\theta_{u,W/D,EC8\_fun,conf} \leq 1/d_{W/D} \tag{A13}$$

$$\mu_{\theta,W/D,EC8\_fun,unconf} \approx b_{W/D} \cdot d_{W/D}{}^2 \tag{A14}$$

$$\mu_{\theta,W/D,EC8\_fun,conf} \approx 1 \tag{A15}$$

If the EC8-3 pure experimental approach is considered, the relationship between θ_u can be expressed as in Equation (A16), and thus is always higher for WB than DB regardless of b_w. Similar confinement contribution is considered for WB and DB, although it may be higher for WB when design in DCH and EC2 provisions are considered [7], and $h_{b,W/D} \approx d_{W/D}$. The subsequent ductility ratio is obtained in Equation (A17). Hence, for confined sections, lower $\theta_{u,W/D}$ and $\mu_{\theta,W/D}$ values are expected according to the experimental approach rather than the fundamental one.

$$\theta_{u,W/D,EC8\_emp} = d_{W/D}{}^{-0.35} \tag{A16}$$

$$\mu_{\theta,W/D,EC8\_emp,conf} = d_{W/D}{}^{0.65} \tag{A17}$$

Appendix B. Characteristics of the Database of Members and Original Formulations in the Base of Eurocode 8 Part 3

Within the original database of specimens which is the basis of the formulations in EC8-3, 266 members are classified as beams (i.e., no axial load and asymmetric reinforcement). However, in this work, symmetric reinforced members are also considered as beams, as design to DCH usually causes such arrangements [6]. Hence, 314 beams and 634 columns, for a total of 948 members, are intended to share the same type of formulations. However, only 11 columns and 37 beams (which represent fractions of 1% of the columns, 12% of the beams, and 5% of the total amount of specimens) are tested in the parallel direction to the cross-section axe of minimum stiffness.

Not all the experimental deformations are available: for DB, the number of specimens in which ϕ_y, ϕ_u, θ_y, and θ_u are calculated is 163, 136, 257, and 240 out of 277, respectively, and for WB is 35, 36, 37, and 37 out of 37, respectively.

The sub-database of DB is composed of 277 specimens coming from 24 different works in the literature. A total of 190 tests are monotonic while 87 are cyclic; 151 are able to show slippage of reinforcement while 126 do not; 106 show 135°-hooked closed stirrups while 171 show 90° hooks; 149 show stirrup arrangements able to furnish some confinement regardless of the closure of hooks while 128 do not; 233 use hot-rolled ductile steel, 34 use tempcore steel, and only 10 use cold-worked steel.

On the other hand, the sub-database of WB is composed of only 37 tests, of which 36 are monotonic and only one is cyclic, and no dynamic test is included since their capability to reproduce ultimate deformation is limited [23]. Three beams are able to show slippage of reinforcement while 34 do not; three beams show 135°-hooked closed stirrups while 34 show 90° hooks; five beams show stirrup arrangements able to furnish some confinement regardless of the closure of hooks while 32 do not; five beams use hot-rolled ductile steel, eight use tempcore steel, and 24 use cold-worked steel.

Both B&F and P&F models assume a parabola rectangle envelope for concrete, without any tension resistance for cyclic loading, as well as elastic–plastic behaviour of steel for lower strains at ultimate situation, and hardening otherwise. Stress values from the original database are adopted, while strain parameters correspond to EC2 except for ultimate nominal strains and maximum-to-yielding strength ratios of steel. Steel ultimate strains for flexural behaviour are taken as a fraction of the nominal values, more reduced for cyclic loading, as suggested in [26]. Regarding the model for confined concrete behaviour, P&F follow the approach proposed in [33], while B&F adopt a model similar to the current one proposed by EC8-3 but with a different evaluation of maximum stress [26]. In this paper, the latter model is followed; thus, formulations of the P&F model for θ_u depending on ϕ cannot be assessed. Additionally, explicit M-ϕ relations are obtained, conversely to the original models, which carry out simplified procedures.

Curvatures adopted as $\phi_{y,exp}$ are indirect values obtained from experimental M_y in each case, instead of using the explicit values measured in the tests, which are expected to show higher uncertainty due to several inherent problems of deformation measurement [23].

The different formulations for θ and L_{pl} proposed by P&F and B&F are listed in Equations (A18)–(A25). Zero-one parameters a_{old}, a_{cy}, a_{pl}, and a_{sl} refer to 90° closed hooks, cyclic loading, plain bars, and slippage, respectively. Parameters a_{st}, $\alpha_{st,mon}$, $\alpha_{st,cyc}$, and α_{cy} refer to steel class, steel class in monotonic or cyclic tests, and type of loading, respectively; their values can be checked in the original works.

$$\theta_{y,P\&F} = \phi_y \frac{L_V}{3} + a_{sl} \frac{0.25\varepsilon_y d_{bL} f_y}{(d - d\prime)\sqrt{f_c}} + 0.0025 \tag{A18}$$

$$\theta_{y,B\&F} = \phi_y \left(\frac{L_V + a_v z}{3} + a_{sl} \cdot 0.125 d_{bL} \frac{f_y}{\sqrt{f_c}} \right) + 0.0014 \left(1 + 1.5\frac{h_b}{L_V} \right) \tag{A19}$$

$$\theta_{u,P\&F,emp1} = 0.01\alpha_{st}\alpha_{cy} \left(1 + \frac{a_{sl}}{2.3} \right) \left(\frac{\max\{0.01;\omega'\}}{\max\{0.01;\omega\}} f_c \right)^{0.275} \left(\frac{L_V}{h_b} \right)^{0.45} \cdot 1.1^{100\alpha_w} \cdot 1.3^{100\rho_d} \tag{A20}$$

$$\theta_{u,P\&F,emp2} = \begin{cases} 0.01\alpha_{st,mon} \left(1 + \frac{a_{sl}}{8} \right) \left(\frac{\max\{0.01;\omega'\}}{\max\{0.01;\omega\}} \frac{L_V}{h_b} f_c \right)^{0.425} & \text{(monotonic)} \\ 0.01\alpha_{st,cyc} \left(1 + \frac{a_{sl}}{2} \right) \cdot f_c^{0.175} \left(\frac{L_V}{h_b} \right)^{0.4} \cdot 1.1^{100\alpha_w} \cdot 1.3^{100\rho_d} & \text{(cyclic)} \end{cases} \tag{A21}$$

$$\theta_{u,B\&F,emp1} = a_{st} \left[1 - \frac{a_{old}a_{cy}}{6} \left(1 + 0.25a_{pl} \right) \right] \left(1 - 0.43a_{cy} \right) \left(1 + \frac{a_{sl}}{2} \right) \left(\frac{\max\{0.01;\omega'\}}{\max\{0.01;\omega\}} f_c \right)^{0.225} \left(\min\left\{ \frac{L_V}{h_b};9 \right\} \right)^{0.35} \cdot 25^{\alpha_w} \cdot 1.25^{100\rho_d} \tag{A22}$$

$$\theta_{u,B\&F,emp2} = \theta_{y,B\&F} + a_{st}^{pl} \left[1 - \frac{a_{old}a_{cy}}{6} \left(1 - 0.05a_{pl} \right) \right] \left(1 - 0.52a_{cy} \right) \left(1 + \frac{5}{8}a_{sl} \right) \left(\frac{\max\{0.01;\omega'\}}{\max\{0.01;\omega\}} \right)^{0.3} f_c^{0.2} \left(\min\left\{ \frac{L_V}{h_b};9 \right\} \right)^{0.35} 25^{\alpha_w} \cdot 1.275^{100\rho_d} \tag{A23}$$

$$\theta_{u,B\&F,fun} = \theta_{y,B\&F} + \left(\phi_u - \phi_y \right) L_{pl,B\&F} \left(1 - \frac{L_{pl,B\&F}}{2L_V} \right) + a_{sl} \left(9.5 - 4a_{cy} \right) d_{bL}\phi_u \tag{A24}$$

$$L_{pl,B\&F} = \begin{cases} 0.04\min\{L_V; 9h_b\} + 1.1h_b \text{ (monotonic)} \\ 0.0\widehat{6}\min\{L_V; 9h_b\} + 0.2h_b \text{ (cyclic, seismic design)} \end{cases} \quad (A25)$$

References

1. Vielma, J.C.; Barbat, A.H.; Oller, S. Seismic safety of low ductility structures used in Spain. *Bull. Earthq. Eng.* **2010**, *8*, 135–155. [CrossRef]
2. Benavent-Climent, A.; Zahran, R. An energy-based procedure for the assessment of seismic capacity of existing frames: Application to RC wide beam systems in Spain. *Soil Dyn. Earthq. Eng.* **2010**, *30*, 354–367. [CrossRef]
3. De Luca, F.; Verderame, G.M.; Gómez-Martínez, F.; Pérez-García, A. The structural role played by masonry infills on RC building performances after the 2011 Lorca, Spain, earthquake. *Bull. Earthq. Eng.* **2014**, *12*, 1999–2026. [CrossRef]
4. López-Almansa, F.; Domínguez, D.; Benavent-Climent, A. Vulnerability analysis of RC buildings with wide beams located in moderate seismicity regions. *Eng. Struct.* **2013**, *46*, 687–702. [CrossRef]
5. Requena-García-Ruiz, M.V.; Morales-Esteban, A.; Durand-Neyra, P.; Zapico-Blanco, B. Influence of the constructive features of RC existing buildings in their ductility and seismic performance. *Bull. Earthq. Eng.* **2021**, *19*, 377–401. [CrossRef]
6. Gómez-Martínez, F. FAST Simplified Vulnerability Approach for Seismic Assessment of Infilled RC MRF Buildings and Its Application to the 2011 Lorca (Spain) Earthquake. Ph.D. Thesis, Technical University of Valencia, Valencia, Spain, 2015. Available online: https://riunet.upv.es/handle/10251/54780 (accessed on 8 November 2022).
7. Gómez-Martínez, F.; Alonso-Durá, A.; De Luca, F.; Verderame, G.M. Ductility of wide-beam RC frames as lateral resisting system. *Bull. Earthq. Eng.* **2016**, *14*, 1545–1569. [CrossRef]
8. Gómez-Martínez, F.; Alonso-Durá, A.; De Luca, F.; Verderame, G.M. Seismic performances and behaviour factor of wide-beam and deep-beam RC frames. *Eng. Struct.* **2016**, *125*, 107–123. [CrossRef]
9. Quintero-Febres, C.G.; Wight, J.K. *Investigation on the Seismic Behavior of RC Interior Wide Beam-Column Connections*; Report No. UMCEE 97-15; Department of Civil and Environmental Engineering, University of Michigan: Ann Arbor, MI, USA, 1997.
10. Benavent-Climent, A. Seismic behavior of RC side beam-column connections under dynamic loading. *J. Earthq. Eng.* **2007**, *11*, 493–511. [CrossRef]
11. Benavent-Climent, A.; Cahís, X.; Zahran, R. Exterior wide beam-column connections in existing RC frames subjected to lateral earthquake loads. *Eng. Struct.* **2009**, *31*, 1414–1424. [CrossRef]
12. Benavent-Climent, A.; Cahís, X.; Vico, J.M. Interior wide beam-column connections in existing RC frames subjected to lateral earthquake loading. *Bull. Earthq. Eng.* **2010**, *8*, 401–420. [CrossRef]
13. Li, B.; Kulkarni, S.A. Seismic behavior of reinforced concrete exterior wide beam-column joints. *J. Or Struct. Eng. (ASCE)* **2010**, *136*, 26–36. [CrossRef]
14. Fadwa, I.; Ali, T.A.; Nazih, E.; Sara, M. Reinforced concrete wide and conventional beam-column connections subjected to lateral load. *Eng. Struct.* **2014**, *76*, 34–48. [CrossRef]
15. Mirzabagheri, S.; Tasnimi, A.A.; Soltani Mohammadi, M. Behavior of interior RC wide and conventional beam-column roof joints under cyclic load. *Eng. Struct.* **2016**, *111*, 333–344. [CrossRef]
16. Behnam, H.; Kuang, J.S.; Samali, B. Parametric finite element analysis of RC wide beam-column connections. *Comput. Struct.* **2018**, *205*, 28–44. [CrossRef]
17. Mirzabagheri, S.; Tasnimi, A.A.; Issa, F. Experimental and numerical study of reinforced concrete interior wide beam-column joints subjected to lateral load. *Can. J. Civ. Eng.* **2018**, *45*, 945–957. [CrossRef]
18. Huang, R.Y.C.; Kuang, J.S.; Behnam, H. Shear strength of exterior wide beam-column joints with different beam reinforcement ratios. *J. Earthq. Eng.* **2018**, *25*, 918–940. [CrossRef]
19. Behnam, H.; Kuang, J.S. Exterior RC wide beam-column connections: Effect of spandrel beam on seismic behavior. *J. Struct. Eng.* **2018**, *144*, 04018013. [CrossRef]
20. *EN 1998-1:2003*; Eurocode 8: Design of Structures for Earthquake Resistance–Part 1: General Rules, Seismic Actions and Rules for Buildings. Comité Européen de Normalisation: Brussels, Belgium, 2004.
21. *ASCE/SEI 41-06*; Seismic Rehabilitation of Existing Buildings. American Society of Civil Engineers: Reston, VA, USA, 2007.
22. *EN 1998-1:2005*; Eurocode 8: Design of Structures for Earthquake Resistance–Part 3: Assessment and Retrofitting of Buildings. Comité Européen de Normalisation: Brussels, Belgium, 2005.
23. Panagiotakos, T.B.; Fardis, M.N. Deformations of reinforced concrete members at yielding and ultimate. *ACI Struct. J.* **2001**, *98*, 135–148.
24. Biskinis, D.E. Resistance and Deformation Capacity of Concrete Members with or without Retrofitting. Ph.D. Thesis, Civil Engineering Department, University of Patras, Patras, Greece, 2007. (In Greek).
25. Biskinis, D.E.; Fardis, M.N. Deformations at flexural yielding of members with continuous or lap-spliced bars. *Struct. Concr.* **2010**, *11*, 127–138. [CrossRef]
26. Biskinis, D.E.; Fardis, M.N. Flexure-controlled ultimate deformations of members with continuous or lap-spliced bars. *Struct. Concr.* **2010**, *11*, 93–108. [CrossRef]
27. Paulay, T.; Priestley, M.J.N. *Seismic Design of Concrete and Masonry Structures*; John Wiley and Sons: New York, NY, USA, 1992.

28. Moehle, J.P.; Hooper, J.D.; Lubke, C.D. *Seismic Design of Reinforced Concrete Special Moment Frames: A Guide for Practicing Engineers*; NEHRP Seismic Design Technical Brief no. 1, NIST GCR 8-917-1; US Department of Commerce, Technology Administration, National Institute of Standards and Technology: Gaithersburg, MD, USA, 2008.

29. Verderame, G.M.; Ricci, P.; Manfredi, G.; Cosenza, E. Ultimate chord rotation of RC columns with smooth bars: Some considerations about EC8 prescriptions. *Bull. Earthq. Eng.* **2010**, *8*, 1351–1373. [CrossRef]

30. *EN 1992-1-1*; Eurocode 2: Design of Concrete Structures: Part 1-1: General Rules and Rules for Buildings. British Standards Institutions: London, UK, 2004.

31. Elwood, K.J.; Matamoros, A.B.; Wallace, J.W.; Lehman, D.E.; Heintz, J.A.; Mitchell, A.D.; Moore, M.; Valley, M.; Lowes, L.N.; Comartin, C.; et al. Update to ASCE/SEI 41 concrete provisions. *Earthq. Spectra* **2007**, *23*, 493–523. [CrossRef]

32. Chung, Y.M.W. Confinement of Rectangular Reinforced Concrete Columns with Non-Seismic Detailing. Ph.D. Thesis, Hong Kong Polytechnic University, Hong Kong, China, 2010.

33. Mander, J.B.; Priestley, M.J.N.; Park, R. Theoretical stress-strain model for confined condrete. *J. Struct. Eng.* **1988**, *114*, 1804–1826. [CrossRef]